knockout mice, proliferation of chondrocytes was decreased, while differentiation was accelerated (67). Since then, an increasing number of specific miRNAs has been identified to have roles in chondrocyte differentiation. Mice lacking miR-140 showed a mild short stature and age-related osteoarthritis-like changes, suggesting that miR-140 regulates both the development and homeostasis of cartilage (68). miR-145 was reported to directly target Sox9 and regulate chondrogenic differentiation of mesenchymal stem cells (69), while miR-199a was shown to be responsive to BMP and to regulate chondrogenesis by targeting Smad1 (70). These findings indicate the importance of miRNA-mediated regulation of chondrogenesis.

Conclusion

In this review, I have overviewed the current knowledge concerning the molecular mechanisms underlying the development of growth cartilage. The proliferation and differentiation of chondrocytes is elaborately controlled by various factors, and their defects are often associated with growth failure and skeletal dysplasias. Further clarification of the molecular basis of cartilage development may lead to the discovery of new therapeutic targets for these conditions.

References

1. Wagner EF, Karsenty G. Genetic control of skeletal development. Curr Opin Genet Dev 2001;11: 527–32. [Medline] [CrossRef]
2. Kronenberg HM. Developmental regulation of the growth plate. Nature 2003;423: 332–6. [Medline] [CrossRef]
3. Michigami T. Regulatory mechanisms for the development of growth plate cartilage. Cell Mol Life Sci 2013: [CrossRef]. [Medline]
4. Zelzer E, Mamluk R, Ferrara N, Johnson RS, Schipani E, Olsen BR. VEGFA is necessary for chondrocyte survival during bone development. Development 2004;131: 2161–71. [Medline] [CrossRef]
5. Stickens D, Behonick DJ, Ortega N, Heyer B, Hartenstein B, Yu Y, *et al.* Altered endochondral bone development in matrix metalloproteinase 13-deficient mice. Development 2004;131: 5883–95. [Medline] [CrossRef]
6. Foster JW, Dominguez-Steglich MA, Guioli S, Kwok C, Weller PA, Stevanovic M, *et al.* Campomelic dysplasia and autosomal sex reversal caused by mutations in an SRY-related gene. Nature 1994;372: 525–30. [Medline] [CrossRef]
7. Wagner T, Wirth J, Meyer J, Zabel B, Held M, Zimmer J, *et al.* Autosomal sex reversal and campomelic dysplasia are caused by mutations in and around the SRY-related gene SOX9. Cell 1994;79: 1111–20. [Medline] [CrossRef]
8. Akiyama H, Lefebvre V. Unraveling the transcriptional regulatory machinery in chondrogenesis. J Bone Miner Metab 2011;29: 390–5. [Medline] [CrossRef]
9. Lefebvre V, Huang W, Harley VR, Goodfellow PN, de Crombrugghe B. SOX9 is a potent activator of the chondrocyte-specific enhancer of the pro alpha1(II) collagen gene. Mol Cell Biol 1997;17: 2336–46. [Medline]
10. Lefebvre V, Li P, de Crombrugghe B. A new long form of Sox5 (L-Sox5), Sox6 and Sox9 are coexpressed in chondrogenesis and cooperatively activate the type II collagen gene. EMBO J 1998;17: 5718–33. [Medline] [CrossRef]
11. Akiyama H, Chaboissier MC, Martin JF, Schedl A, de Crombrugghe B. The transcription factor Sox9 has essential roles in successive steps of the chondrocyte differentiation pathway and is required for expression of Sox5 and Sox6. Genes Dev 2002;16: 2813–28. [Medline] [CrossRef]
12. Vale-Cruz DS, Ma Q, Syme J, LuValle PA. Activating transcription factor-2 affects skeletal growth by modulating pRb gene expression. Mech Dev 2008;125: 843–56. [Medline] [CrossRef]
13. Wang ZQ, Ovitt C, Grigoriadis AE, Mohle-Steinlein U, Ruther U, Wagner EF. Bone and haematopoietic defects in mice lacking c-fos. Nature 1992;360: 741–5. [Medline] [CrossRef]
14. Yoshida CA, Komori T. Role of Runx proteins in chondrogenesis. Crit Rev Eukaryot Gene Expr 2005;15: 243–54. [Medline] [CrossRef]

15. Yoshida CA, Yamamoto H, Fujita T, Furuichi T, Ito K, Inoue K, *et al.* Runx2 and Runx3 are essential for chondrocyte maturation, and Runx2 regulates limb growth through induction of Indian hedgehog. Genes Dev 2004;18: 952–63. [Medline] [CrossRef]
16. Selvamurugan N, Kwok S, Partridge NC. Smad3 interacts with JunB and Cbfa1/Runx2 for transforming growth factor-beta1-stimulated collagenase-3 expression in human breast cancer cells. J Biol Chem 2004;279: 27764–73. [Medline] [CrossRef]
17. Zheng Q, Zhou G, Morello R, Chen Y, Garcia-Rojas X, Lee B. Type X collagen gene regulation by Runx2 contributes directly to its hypertrophic chondrocyte-specific expression in vivo. J Cell Biol 2003;162: 833–42. [Medline] [CrossRef]
18. Dy P, Wang W, Bhattaram P, Wang Q, Wang L, Ballock RT, *et al.* Sox9 directs hypertrophic maturation and blocks osteoblast differentiation of growth plate chondrocytes. Dev Cell 2012;22: 597–609. [Medline] [CrossRef]
19. Hinoi E, Bialek P, Chen YT, Rached MT, Groner Y, Behringer RR, *et al.* Runx2 inhibits chondrocyte proliferation and hypertrophy through its expression in the perichondrium. Genes Dev 2006;20: 2937–42. [Medline] [CrossRef]
20. Arnold MA, Kim Y, Czubryt MP, Phan D, McAnally J, Qi X, *et al.* MEF2C transcription factor controls chondrocyte hypertrophy and bone development. Dev Cell 2007;12: 377–89. [Medline] [CrossRef]
21. Kozhemyakina E, Cohen T, Yao TP, Lassar AB. Parathyroid hormone-related peptide represses chondrocyte hypertrophy through a protein phosphatase 2A/histone deacetylase 4/MEF2 pathway. Mol Cell Biol 2009;29: 5751–62. [Medline] [CrossRef]
22. Satokata I, Ma L, Ohshima H, Bei M, Woo I, Nishizawa K, *et al.* Msx2 deficiency in mice causes pleiotropic defects in bone growth and ectodermal organ formation. Nat Genet 2000;24: 391–5. [Medline] [CrossRef]
23. Amano K, Ichida F, Sugita A, Hata K, Wada M, Takigawa Y, *et al.* MSX2 stimulates chondrocyte maturation by controlling Ihh expression. J Biol Chem 2008;283: 29513–21. [Medline] [CrossRef]
24. Karreth F, Hoebertz A, Scheuch H, Eferl R, Wagner EF. The AP1 transcription factor Fra2 is required for efficient cartilage development. Development 2004;131: 5717–25. [Medline] [CrossRef]
25. Ionescu A, Kozhemyakina E, Nicolae C, Kaestner KH, Olsen BR, Lassar AB. FoxA family members are crucial regulators of the hypertrophic chondrocyte differentiation program. Dev Cell 2012;22: 927–39. [Medline] [CrossRef]
26. Schipani E, Ryan HE, Didrickson S, Kobayashi T, Knight M, Johnson RS. Hypoxia in cartilage: HIF-1alpha is essential for chondrocyte growth arrest and survival. Genes Dev 2001;15: 2865–76. [Medline]
27. Maes C, Araldi E, Haigh K, Khatri R, Van Looveren R, Giacia AJ, *et al.* VEGF-independent cell-autonomous functions of HIF-1alpha regulating oxygen consumption in fetal cartilage are critical for chondrocyte survival. J Bone Miner Res 2012;27: 596–609. [Medline] [CrossRef]
28. Ornitz DM. FGF signaling in the developing endochondral skeleton. Cytokine Growth Factor Rev 2005;16: 205–13. [Medline] [CrossRef]
29. Rousseau F, Bonaventure J, Legeai-Mallet L, Pelet A, Rozet JM, Maroteaux P, *et al.* Mutations in the gene encoding fibroblast growth factor receptor-3 in achondroplasia. Nature 1994;371: 252–4. [Medline] [CrossRef]
30. Bellus GA, McIntosh I, Smith EA, Aylsworth AS, Kaltlla I, Horton WA, *et al.* A recurrent mutation in the tyrosine kinase domain of fibroblast growth factor receptor 3 causes hypochondroplasia. Nat Genet 1995;10: 357–9. [Medline] [CrossRef]
31. Tavormina PL, Shiang R, Thompson LM, Zhu YZ, Wilkin DJ, Lachman RS, *et al.* Thanatophoric dysplasia (types I and II) caused by distinct mutations in fibroblast growth factor receptor 3. Nat Genet 1995;9: 321–8. [Medline] [CrossRef]
32. Deng C, Wynshaw-Boris A, Zhou F, Kuo A, Leder P. Fibroblast growth factor receptor 3 is a negative regulator of bone growth. Cell 1996;84: 911–21. [Medline] [CrossRef]
33. Peters K, Ornitz D, Werner S, Williams L. Unique expression pattern of the FGF receptor 3 gene during mouse organogenesis. Dev Biol 1993;155: 423–30. [Medline] [CrossRef]

34. Peters KG, Werner S, Chen G, Williams LT. Two FGF receptor genes are differentially expressed in epithelial and mesenchymal tissues during limb formation and organogenesis in the mouse. Development 1992;114: 233–43. [Medline]
35. Chen L, Adar R, Yang X, Monsonego EO, Li C, Hauschka PV, *et al.* Gly369Cys mutation in mouse FGFR3 causes achondroplasia by affecting both chondrogenesis and osteogenesis. J Clin Invest 1999;104: 1517–25. [Medline] [CrossRef]
36. Dailey L, Laplantine E, Priore R, Basilico C. A network of transcriptional and signaling events is activated by FGF to induce chondrocyte growth arrest and differentiation. J Cell Biol 2003;161: 1053–66. [Medline] [CrossRef]
37. Li C, Chen L, Iwata T, Kitagawa M, Fu XY, Deng CX. A Lys644Glu substitution in fibroblast growth factor receptor 3 (FGFR3) causes dwarfism in mice by activation of STATs and ink4 cell cycle inhibitors. Hum Mol Genet 1999;8: 35–44. [Medline] [CrossRef]
38. Ohbayashi N, Shibayama M, Kurotaki Y, Imanishi M, Fujimori T, Itoh N, *et al.* FGF18 is required for normal cell proliferation and differentiation during osteogenesis and chondrogenesis. Genes Dev 2002;16: 870–9. [Medline] [CrossRef]
39. Liu Z, Xu J, Colvin JS, Ornitz DM. Coordination of chondrogenesis and osteogenesis by fibroblast growth factor 18. Genes Dev 2002;16: 859–69. [Medline] [CrossRef]
40. Kronenberg HM. PTHrP and skeletal development. Ann NY Acad Sci 2006;1068: 1–13. [Medline] [CrossRef]
41. St-Jacques B, Hammerschmidt M, McMahon AP. Indian hedgehog signaling regulates proliferation and differentiation of chondrocytes and is essential for bone formation. Genes Dev 1999;13: 2072–86. [Medline] [CrossRef]
42. Kobayashi T, Soegiarto DW, Yang Y, Lanske B, Schipani E, McMahon AP, *et al.* Indian hedgehog stimulates periarticular chondrocyte differentiation to regulate growth plate length independently of PTHrP. J Clin Invest 2005;115: 1734–42. [Medline] [CrossRef]
43. Mak KK, Kronenberg HM, Chuang PT, Mackem S, Yang Y. Indian hedgehog signals independently of PTHrP to promote chondrocyte hypertrophy. Development 2008;135: 1947–56. [Medline] [CrossRef]
44. Chusho H, Tamura N, Ogawa Y, Yasoda A, Suda M, Miyazawa T, *et al.* Dwarfism and early death in mice lacking C-type natriuretic peptide. Proc Natl Acad Sci USA 2001;98: 4016–21. [Medline] [CrossRef]
45. Yasoda A, Ogawa Y, Suda M, Tamura N, Mori K, Sakuma Y, *et al.* Natriuretic peptide regulation of endochondral ossification. Evidence for possible roles of the C-type natriuretic peptide/guanylyl cyclase-B pathway. J Biol Chem 1998;273: 11695–700. [Medline] [CrossRef]
46. Yasoda A, Komatsu Y, Chusho H, Miyazawa T, Ozasa A, Miura M, *et al.* Overexpression of CNP in chondrocytes rescues achondroplasia through a MAPK-dependent pathway. Nat Med 2004;10: 80–6. [Medline] [CrossRef]
47. Bartels CF, Bukulmez H, Padayatti P, Rhee DK, van Ravenswaaji-Arts C, Pauli RM, *et al.* Mutations in the transmembrane natriuretic peptide receptor NPR-B impair skeletal growth and cause acromesomelic dysplasia, type Maroteaux. Am J Hum Genet 2004;75: 27–34. [Medline] [CrossRef]
48. Hachiya R, Ohashi Y, Kamei Y, Suganami T, Mochizuki H, Mitsui N, *et al.* Intact kinase homology domain of natriuretic peptide receptor-B is essential for skeletal development. J Clin Endocrinol Metab 2007;92: 4009–14. [Medline] [CrossRef]
49. Miura K, Namba N, Fujiwara M, Ohata Y, Ishida H, Kitaoka T, *et al.* An overgrowth disorder associated with excessive production of cGMP due to a gain-of-function mutation of the natriuretic peptide receptor 2 gene. PLoS One 2012;7: e42180. [Medline] [CrossRef]
50. Ulici V, Hoenselaar KD, Gillespie JR, Beier F. The PI3K pathway regulates endochondral bone growth through control of hypertrophic chondrocyte differentiation. BMC Dev Biol 2008;8: 40. [Medline] [CrossRef]
51. Pogue R, Lyons K. BMP signaling in the cartilage growth plate. Curr Top Dev Biol 2006;76: 1–48. [Medline] [CrossRef]
52. Mackie EJ, Ahmed YA, Tatarczuch L, Chen KS, Mirams M. Endochondral ossification: how

cartilage is converted into bone in the developing skeleton. Int J Biochem Cell Biol 2008;40: 46–62. [Medline] [CrossRef]
53. Olney RC, Mougey EB. Expression of the components of the insulin-like growth factor axis across the growth-plate. Mol Cell Endocrinol 1999;156: 63–71. [Medline] [CrossRef]
54. Tavella S, Raffo P, Tacchetti C, Cancedda R, Castagnola P. N-CAM and N-cadherin expression during in vitro chondrogenesis. Exp Cell Res 1994;215: 354–62. [Medline] [CrossRef]
55. Oberlender SA, Tuan RS. Expression and functional involvement of N-cadherin in embryonic limb chondrogenesis. Development 1994;120: 177–87. [Medline]
56. ffrench-Constant C, Colognato H. Integrins: versatile integrators of extracellular signals. Trends Cell Biol 2004;14: 678–86. [Medline] [CrossRef]
57. Loeser RF. Chondrocyte integrin expression and function. Biorheology 2000;37: 109–16. [Medline]
58. Aszodi A, Hunziker EB, Brakebusch C, Fassler R. Beta1 integrins regulate chondrocyte rotation, G1 progression, and cytokinesis. Genes Dev 2003;17: 2465–79. [Medline] [CrossRef]
59. Terpstra L, Prud'homme J, Arabian A, Takeda S, Karsenty G, Dedhar S, *et al.* Reduced chondrocyte proliferation and chondrodysplasia in mice lacking the integrin-linked kinase in chondrocytes. J Cell Biol 2003;162: 139–48. [Medline] [CrossRef]
60. Mertz EL, Facchini M, Pham AT, Gualeni B, De Leonardis F, Rossi A, *et al.* Matrix disruptions, growth, and degradation of cartilage with impaired sulfation. J Biol Chem 2012;287: 22030–42. [Medline] [CrossRef]
61. Sato T, Kudo T, Ikehara Y, Ogawa H, Hirano T, Kiyohara K, *et al.* Chondroitin sulfate N-acetylgalactosaminyltransferase 1 is necessary for normal endochondral ossification and aggrecan metabolism. J Biol Chem 2011;286: 5803–12. [Medline] [CrossRef]
62. Settembre C, Arteaga-Solis E, McKee MD, de Pablo R, Al Awqati Q, Ballabio A, *et al.* Proteoglycan desulfation determines the efficiency of chondrocyte autophagy and the extent of FGF signaling during endochondral ossification. Genes Dev 2008;22: 2645–50. [Medline] [CrossRef]
63. Koshimizu T, Kawai M, Kondou H, Tachikawa K, Sakai N, Ozono K, *et al.* Vinculin functions as regulator of chondrogenesis. J Biol Chem 2012;287: 15760–75. [Medline] [CrossRef]
64. Vega RB, Matsuda K, Oh J, Barbosa AC, Yang X, Meadows E, *et al.* Histone deacetylase 4 controls chondrocyte hypertrophy during skeletogenesis. Cell 2004;119: 555–66. [Medline] [CrossRef]
65. Hong S, Derfoul A, Pereira-Mouries L, Hall DJ. A novel domain in histone deacetylase 1 and 2 mediates repression of cartilage-specific genes in human chondrocytes. FASEB J 2009;23: 3539–52. [Medline] [CrossRef]
66. Zimmermann P, Boeuf S, Dickhut A, Boehmer S, Olek S, Richter W. Correlation of COL10A1 induction during chondrogenesis of mesenchymal stem cells with demethylation of two CpG sites in the COL10A1 promoter. Arthritis Rheum 2008;58: 2743–53. [Medline] [CrossRef]
67. Kobayashi T, Lu J, Cobb BS, Rodda SJ, McMahon AP, Schipani E, *et al.* Dicer-dependent pathways regulate chondrocyte proliferation and differentiation. Proc Natl Acad Sci USA 2008;105: 1949–54. [Medline] [CrossRef]
68. Miyaki S, Sato T, Inoue A, Otsuki S, Ito Y, Yokoyama S, *et al.* MicroRNA-140 plays dual roles in both cartilage development and homeostasis. Genes Dev 2010;24: 1173–85. [Medline] [CrossRef]
69. Yang B, Guo H, Zhang Y, Chen L, Ying D, Dong S. MicroRNA-145 regulates chondrogenic differentiation of mesenchymal stem cells by targeting Sox9. PLoS One 2011;6: e21679. [Medline] [CrossRef]
70. Lin EA, Kong L, Bai XH, Luan Y, Liu CJ. miR-199a, a bone morphogenic protein 2-responsive MicroRNA, regulates chondrogenesis via direct targeting to Smad1. J Biol Chem 2009;284: 11326–35. [Medline] [CrossRef]

腎と骨代謝 2012 Vol. 25 No. 2

8

遺伝子異常と骨硬化性疾患

道上 敏美*

要旨 骨硬化性疾患は骨吸収の障害あるいは骨形成の亢進により引き起こされる．骨吸収の障害は大理石骨病やpycnodysostosisなどの類縁疾患を引き起こす．大理石骨病はさまざまな重症度を示す異質性の高い疾患であり，近年，多くの分子が責任分子として同定されている．重症型である常染色体劣性大理石骨病は破骨細胞機能に関わる遺伝子（*TCIRG1*, *CLCN7*, *OSTM1*）の障害により引き起こされるosteoclast-richな病型と，破骨細胞形成に関わる遺伝子（*TNFSF11*, *TNFRSF11A*）の障害に起因するosteoclast-poorな病型に分類される．遺伝性骨硬化性疾患は稀少であるが，その病態の解析は骨量制御メカニズムの解明に寄与し，骨粗鬆症などの一般的な代謝性骨疾患の新規治療法の開発にもつながる．

〈Key point〉

はじめに

骨硬化性疾患は骨吸収の障害あるいは骨形成の亢進により引き起こされる．骨吸収障害による代表的な骨硬化性疾患が大理石骨病であり，種々の遺伝子異常により引き起こされる異質性の高い疾患である．また，骨形成の亢進による骨硬化性疾患のなかにはWntシグナルやTGF-βシグナルの構成因子の異常に基づくものが存在し，骨量制御におけるこれらのシグナルの重要性を示唆する．

本稿においては，骨硬化を示す多様な遺伝性疾患のうち主要な疾患の分子病態について，最近の知見を概説する．

Ⅰ．骨吸収の障害に伴う骨硬化性疾患

破骨細胞の分化や活性化，生存には多くの分子が関与するが，とくに骨芽細

Key words：大理石骨病，骨吸収障害，骨形成亢進，遺伝子異常

* 地方独立行政法人大阪府立病院機構大阪府立母子保健総合医療センター研究所環境影響部門
（〒594-1101 大阪府和泉市室堂町840）

表　大理石骨病および類縁疾患の責任分子と表現型

責任遺伝子	蛋白質	機　能	病　型
TCIRG1	プロトンポンプ a3 subunit	吸収窩の酸性化	ARO
CLCN7	ClC-7	吸収窩の酸性化	ARO, IARO, ADO Ⅱ
OSTM1	OSTM1	ClC-7 の β subunit	ARO
CA2	Carbonic anhydrase Ⅱ	細胞内の酸性化	IARO
PLEKHM1	PLEKHM1	小胞輸送	IARO
TNFSF11	RANKL	破骨細胞の形成，活性化，生存	ARO
TNFRSF11A	RANK	破骨細胞の形成，活性化，生存	ARO
IKBKG	NEMO	NF-κB シグナルに関与	OL-EDA-ID
CTSK	Cathepsin K	蛋白分解酵素	pycnodysostosis

ARO：autosomal recessive osteopetrosis
IARO：intermediate-type of autosomal recessive osteopetrosis
ADO Ⅱ：autosomal dominant osteopetrosis, type Ⅱ
OL-EDA-ID：ectodermal dysplasia, anhidrotic, with immunodeficiency, osteopetrosis, and lymphedema

胞系列の細胞が発現する receptor activator of nuclear factor κ B ligand（RANKL）と前破骨細胞や破骨細胞に発現する受容体である RANK との相互作用が中心的な役割を果たしている．成熟破骨細胞は極性を有し，骨に接着する．骨への接着部の内部の形質膜は波状縁を形成し，この領域（吸収窩）ではライソゾーム酵素であるカテプシン K や酸が分泌され，活発に骨が吸収される．こうした酵素や酸の産生，分泌過程の異常は骨吸収の障害をきたし，大理石骨病（osteopetrosis）や pycnodysostosis などの骨硬化性疾患を引き起こす[1),2)]．

RANKL
RANK
カテプシン K
酸

大理石骨病は異質性が高く，予後不良な常染色体劣性乳児型（乳児悪性型）と軽症の常染色体優性成人型（遅発型）が主要な病型であるが，中間型や，尿細管性アシドーシスを伴う型，免疫異常を伴う型も存在する．表に，骨吸収障害による骨硬化性疾患の責任分子をまとめた．各疾患の分子病態について以下に記述する．

1．常染色体劣性乳児型大理石骨病

乳児悪性型大理石骨病（infantile malignant osteopetrosis）とも呼ばれる予後不良な病型である．びまん性骨硬化を示し，骨のモデリングとリモデリングがともに障害される．乳児期早期に大頭症，進行性難聴および視力障害，肝脾腫，重度の貧血で発症する．難聴，視力障害は神経管狭小化による神経圧迫症状として出現し，貧血は骨髄腔の狭小化による．汎血球減少を呈するため感染や出血を起こしやすく，治療が行われなければ幼児期までに死亡することが多

い．

5遺伝子が同定

乳児悪性型大理石骨病の責任遺伝子として，これまでに5遺伝子が同定されている．空胞型プロトンポンプa3サブユニットをコードする *TCIRG1*[3]，クロライドチャネルをコードする *CLCN7*[4]，マウスの *grey-lethal* のヒトオルソログである *OSTM1*[5]，RANKLをコードする *TNFSF11*[6]，RANKをコードする *TNFRSF11A*[7] である．

1) *TCIRG1*

OMIM

OPTB1

a3サブユニット

プロトン

破骨細胞機能異常

乳児悪性型大理石骨病の50%以上は *TCIRG1* 遺伝子のホモあるいは複合ヘテロ変異により引き起され，Online Mendelian Inheritance in Man（OMIM）では［osteopetrosis, autosomal recessive 1；OPTB1, #259700］と分類されている．*TCIRG1* がコードするa3サブユニットは成熟破骨細胞の波状縁に高発現しており，プロトン（H^+）を輸送することにより吸収窩の酸性化に関与する．本遺伝子の変異による大理石骨病の骨組織においては，破骨細胞数はむしろ増加しているが，これらの破骨細胞においては波状縁が形成されておらず，破骨細胞機能異常の存在がうかがえる[8]．

2) *CLCN7*

OPTB4

ClC-7

OSTM1

OPTB5

乳児悪性型大理石骨病のうち，*CLCN7* 遺伝子のホモまたは複合ヘテロ変異により引き起こされる症例は10～15％程度存在し，神経変性を伴うことがある[1]．OMIMでは［osteopetrosis, autosomal recessive 4；OPTB4, #611490］と分類されている．*CLCN7* がコードするClC-7は空胞型プロトンポンプとともに骨吸収窩の酸性化に関わる．また，Chalhoubら[5]は，きわめて重症の大理石骨病を呈する自然発症変異マウス *gl/gl* の責任遺伝子として *grey-lethal* を同定し，そのヒトオルソログ *OSTM1* の変異がヒトにおいても重篤な常染色体劣性遺伝性大理石骨病を引き起こすことを報告した［osteopetrosis, autosomal recessive 5；OPTB5, OMIM #259720］．OSTM1はClC-7と協調して働くと考えられている[9]．

3) *TNFSF11*, *TNFRSF11A*

osteoclast-rich

RANKL

OPTB2

RANK

OPTB7

osteoclast-poor

TCIRG1, *CLCN7*, *OSTM1* の変異による大理石骨病においては，破骨細胞の機能が障害されているが形成には異常がないため，骨組織における破骨細胞数はむしろ増加しており，osteoclast-rich osteopetrosisと呼ばれる．一方，RANKLをコードする *TNFSF11* の変異に基づく大理石骨病［osteopetrosis, autosomal recessive 2；OPTB2, OMIM #259710］や，RANKをコードする *TNFRSF11A* 遺伝子の変異による大理石骨病［osteopetrosis, autosomal recessive 7；OPTB7, OMIM #612301］においては，骨組織に成熟破骨細胞はほとんど認められず，osteoclast-poor osteopetrosisと称される[10]．

4）治　療

TCIRG1 や *CLCN7*，*TNFRSF11A* など破骨細胞系列の細胞に発現する遺伝子の変異による大理石骨病については，治療として造血幹細胞移植が行われる．一方，*TNFSF11* の変異に基づく大理石骨病においては造血幹細胞移植は無効であり，RANKL のリコンビナント蛋白質の投与が有効である．

2．常染色体優性成人型（遅発型）大理石骨病

常染色体優性大理石骨病は劣性大理石骨病よりも軽症であり，診断に至っていない症例も少なからず存在すると考えられる．従来，X 線所見の違いからⅠ型（ADO Ⅰ）とⅡ型（ADO Ⅱ）に分類されていた．

1）ADO Ⅱ（OPTA2）

ADO Ⅱ［osteopetrosis, autosomal dominant 2；OPTA2, OMIM #166600］においては X 線上全身骨の硬化を認め，rugger-jergey vertebra と表記される椎体終板の硬化像が特徴的である．Albers-Schönberg disease とも呼ばれる．通常，小児期に骨折や下顎の骨髄炎，顔面神経麻痺などで気づかれる．骨吸収の障害のため，未熟骨が成熟した緻密骨に置き換えられず，易骨折性をきたす．本病型は *CLCN7* のヘテロ変異により引き起こされる[11]．

rugger-jergey vertebra

Albers-Schönberg disease

CLCN7

2）ADO Ⅰ（OPTA1）

一方，ADO Ⅰ［osteopetrosis, autosomal dominant 1；OPTA1, OMIM #607634］においては，とくに頭蓋冠の硬化が著明で，長管骨皮質骨の肥厚を示すが，椎体にはほとんど異常を認めない．また，骨折頻度は高くなく，無症状で経過することが多い．2003 年，ADO Ⅰが *LDL receptor-related protein 5*（*LRP5*）の機能獲得型変異に起因することが明らかとなった[12]．このことから，本病型は実際には破骨細胞性骨吸収の障害ではなく，骨芽細胞機能の異常による骨硬化であると推察され，病態的には大理石骨病には当てはまらないと考えられる．

LRP5

骨芽細胞機能異常

3．中間型大理石骨病

本病型は小児期に発症し，骨折や骨髄炎，低身長，軽度～中等度の貧血，髄外造血，歯牙の異常，顔面神経麻痺，難聴などを種々の程度に呈する．生命予後が良いことから，乳児型大理石骨病とは区別されている．

CLCN7

中間型大理石骨病のなかには，*CLCN7* 遺伝子の両アレルの変異により引き起こされる症例が存在する．*CLCN7* の変異がさまざまな重症度の大理石骨病を引き起こすことは興味深く，より詳細な遺伝子型/表現型解析が望まれる．

そのほか，中間型大理石骨病の責任遺伝子の一つとして，2007 年に

PLEKHM1
OPTB6

PLEKHM1 (*Pleckstrin homology domain containing, family M member 1*) 遺伝子が同定され，本病型は［osteopetrosis, autosomal recessive 6；OPTB6, OMIM #611497］と分類された[13]．本遺伝子は，自然発症大理石骨病ラットである *incisors absent* の責任遺伝子でもある．本遺伝子の欠失は破骨細胞の小胞様構造のなかに酒石酸抵抗性フォスファターゼの蓄積をもたらすと報告されているが[13]，本分子の破骨細胞における機能の詳細は不明である．

4．その他の大理石骨病

carbonic anhydrase Ⅱ（CAⅡ）欠損症は，常染色体劣性遺伝形式を示し，脳の石灰化や尿細管性アシドーシスを伴う中間型大理石骨病を呈する［osteopetrosis, autosomal recessive 3；OPTB3, OMIM #259730］．本酵素は H_2CO_3 を産生し，産生された H_2CO_3 は細胞内で H^+ と HCO_3^- に分解されることにより骨吸収に関与する．

OPTB3
H_2CO_3

また，OL-EDA-ID［ectodermal dysplasia, anhidrotic, with immunodeficiency, osteopetrosis, and lymphedema；OMIM #300301］は大理石骨病，リンパ浮腫，anhidrotic ectodermal dysplasia（EDA；無汗症を伴う外胚葉異形成症）を呈し，幼児期に多発性感染症により死亡するまれな伴性劣性遺伝性疾患である．本症候群の責任遺伝子として nuclear factor κB（NF-κB）essential modulator（NEMO）をコードする *IKBKG* 遺伝子が同定されている[14]．

EDA
NF-κB
NEMO
IKBKG

5．Pycnodysostosis

pycnodysostosis［OMIM #265800］は，びまん性骨硬化，四肢短縮型小人症，頭蓋・顔面の形成異常，歯牙形成異常や易骨折性を示す常染色体劣性遺伝性疾患で，カテプシンKをコードする *CTSK* 遺伝子の機能喪失型変異に基づく[15]．破骨細胞数は正常であり，波状縁も形成されているが，個々の破骨細胞周囲の脱灰骨領域が増加している．また，これらの破骨細胞は，コラーゲン線維を含む異常な細胞質内空胞を有する．これらの所見から，本症患者の破骨細胞においては基質蛋白質の分解が障害されていることが示唆される．近年，カテプシンK阻害剤が骨粗鬆症治療薬として期待されている．

カテプシンK
CTSK

Ⅱ．骨形成の亢進に伴う骨硬化性疾患

骨形成亢進に起因する骨硬化性疾患のなかには，以下の遺伝子の変異に基づくものが存在する．

1．*SOST* 遺伝子の変異による疾患

Wnt シグナル

sclerostin

van Buchem disease

常染色体劣性遺伝

sclerosteosis

SOST 遺伝子は Wnt シグナル阻害因子として働く sclerostin をコードする．*SOST* の異常は van Buchem disease［OMIM #239100］や sclerosteosis［OMIM #269500］を引き起こす[16),17)]．van Buchem disease は常染色体劣性遺伝形式を示し，進行性の顎の非対称性拡大や頭蓋骨，鎖骨，肋骨や骨幹部の硬化により特徴づけられる疾患で，*SOST* 遺伝子の下流の enhancer を含む 52-kb が欠失している[16)]．また，sclerosteosis は *SOST* の機能喪失変異に起因し[17)]，van Buchem disease に類似するが合指症を呈し，主として南アフリカに居住するオランダ系移民において認められる．

2．*LRP5* 遺伝子の変異による疾患

low-density lipoprotein receptor related protein 5（LRP5）は Wnt カノニカル経路の共役受容体の一つとして機能する．*LRP5* 遺伝子の機能獲得型変異は骨硬化を示すさまざまな疾患で同定されており，そのなかには endothelial hyperostosis［OMIM #144750］，van Buchem disease type Ⅱ［OMIM #607636］，autosomal dominant osteosclerosis［OMIM #144750］，前述した autosomal dominant osteopetrosis type Ⅰ［ADO Ⅰ；OMIM #607634］が含まれる[12)]．*SOST* の変異に基づく van Buchem disease が常染色体劣性遺伝形式を示すのに対し，*LRP5* の変異に基づく van Buchem disease type Ⅱは常染色体優性遺伝形式を示す．そのほか，遺伝的に高骨量を示す家系においても *LRP5* の機能獲得型変異が同定されている[18)]．LRP5 による骨量制御のメカニズムについては，近年，腸管におけるセロトニン産生抑制を介するとの報告もなされている[19)]．

van Buchem disease type Ⅱ

常染色体優性遺伝

セロトニン

3．TGF-β シグナルの異常による疾患

Camurati-Engelmann disease

LAP

Camurati-Engelmann disease［OMIM #131300］は骨内膜性，骨外膜性両方の膜性骨化の進行を基本所見とする，常染色体優性遺伝形式を示す骨硬化性疾患である．幼児期に筋力低下や歩行異常で気づかれ，四肢の骨痛や易疲労感を示す．2000 年，本疾患が *TGF-β1* 遺伝子変異に基づくことが報告された[20)]．同定された変異は latency-associated peptide（LAP）をコードするエクソンに集中しており，TGF-β1 シグナルの活性化をもたらすことにより骨硬化をきたすと考えられている．*TGF-β1* 遺伝子に変異のない症例は Camurati-En-

gelmann disease type II［OMIM %606631］として分類されている．

おわりに

骨硬化を示す遺伝性骨疾患の分子病態についてまとめた．ここに挙げた疾患はいずれも稀少な疾患であるが，これらの病態を分子レベルで理解することは，骨量制御メカニズムの解明に大きく寄与し，骨粗鬆症をはじめとする一般的な代謝性骨疾患の新規治療法の開発にもつながる．exome sequencingなどの新規手法の導入により，さらなる疾患責任遺伝子の同定が期待される．

文　献

1) Segovia-Silvestre T, Neutzsky-Wulff AV, Sorensen MG, et al : Advances in osteoclast biology resulting from the study of osteopetrotic mutations. Hum Genet 124 : 561-577, 2009
2) Askmyr MK, Fasth A, Richter J : Towards a better understanding and new therapeutics of osteopetrosis. Br J Haematol 140 : 597-609, 2008
3) Frattini A, Orchard PJ, Sobacchi C, et al : Defects in TCIRG1 subunit of the vacuolar proton pump are responsible for a subset of human autosomal recessive osteopetrosis. Nat Genet 25 : 343-346, 2000
4) Kornak U, Kasper D, Bösl MR, et al : Loss of the ClC-7 chloride channel leads to osteopetrosis in mice and man. Cell 104 : 205-215, 2001
5) Chalhoub N, Benachenhou N, Rajapurohitam V, et al : Grey-lethal mutation induces severe malignant autosomal recessive osteopetrosis in mouse and human. Nat Med 9 : 399-406, 2003
6) Sobacchi C, Frattini A, Guerrini MM, et al : Osteoclast-poor human osteopetrosis due to mutations in the gene encoding RANKL. Nat Genet 39 : 960-962, 2007
7) Guerrini MM, Sobacchi C, Cassani B, et al : Human osteoclast-poor osteopetrosis with hypogammaglobinemia due to TNFRSF11A (RANK) mutations. Am J Hum Genet 83 : 64-76, 2008
8) Michigami T, Kageyama T, Satomura K, et al : Novel mutations in the a3 subunit of vacuolar H^+-adenosine triphosphatase in a Japanese patient with infantile malignant osteopetrosis. Bone 30 : 436-439, 2002
9) Lange PF, Wartosch L, Jentsch TJ, et al : ClC-7 requires Ostm1 as a b-subunit to support bone resorption and lysosomal function. Nature 440 : 220-223, 2006
10) Villa A, Guerrini MM, Cassani B, et al : Infantile malignant, autosomal recessive osteopetrosis : the rich and the poor. Calcif Tissue Int 84 : 1-12, 2009
11) Cleiren E, Bénichou O, Van Hul E, et al : Albers-Schönberg disease (autosomal dominant osteopetrosis, type II) results from mutations in the ClCN7 chloride channel gene. Hum Mol Genet 10 : 2861-2867, 2001
12) Van Wesenbeeck L, Cleiren E, Gram J, et al : Six novel mutations in the LDL receptor-related protein 5 (LRP5) gene in different conditions with an increased bone density. Am J Hum Genet 72 : 763-771, 2003
13) Van Wesenbeeck L, Odgren PR, Coxon FP, et al : Involvement of PLEKHM1 in osteoclastic vesicular transport and osteopetrosis in incisors absent rat and humans. J Clin Invest 117 : 919-930, 2007
14) Döffinger R, Smahi A, Bessia C, et al : X-linked anhidrotic ectodermal dysplasia with immunodeficiency is caused by impaired NF-κB signaling. Nat Genet 27 : 277-285, 2001
15) Gelb BD, Shi G-P, Chapman HA, et al : Pycnodysostosis, a lysosomal disease caused by cathepsin K deficiency. Science 273 (5279) : 1236-1238, 1996

16) Loots GG, Kneissel M, Keller H, et al : Genomic deletion of a long-range bone enhancer misregulates sclerostin in van Buchem disease. Genome Res 15 : 928-935, 2005
17) Brunkow ME, Gardner JC, Van Ness J, et al : Bone dysplasia sclerosteosis results from loss of the SOST gene product, a novel cystine knot-containing protein. Am J Hum Genet 68 : 577-589, 2001
18) Boyden LM, Mao J, Belsky J, et al : High bone density due to a mutation in LDL-receptor-related protein 5. N Engl J Med 346 : 1513-1521, 2002
19) Yadav VK, Ryu J-H, Suda N, et al : Lrp5 controls bone formation by inhibiting serotonin synthesis in the duodenum. Cell 135 : 825-837, 2008
20) Kinoshita A, Saito T, Tomita H, et al : Domain-specific mutations in TGFβ1 result in Camurati-Engelmann disease. Nat Genet 26 : 19-20, 2000

Summary

Genetic features of bone sclerosing diseases

Toshimi Michigami*

Sclerosing bone disorders are caused by impaired osteoclastic bone resorption or increased bone formation. Impaired bone resorption results in osteopetrosis and related diseases such as pycnodysostosis. Osteopetrosis is a heterogeneous disease, and various molecules have been recently identified as being responsible. Infantile malignant, autosomal recessive osteopetrosis can be classified into osteoclast-rich and osteoclast-poor forms, which are caused by the dysfunction of osteoclasts and impaired osteoclastogenesis, respectively. Analysis of rare, heritable sclerosing bone disorders contributes to the understanding of molecular mechanisms underlying bone mass control. It may also lead to the development of drugs for common metabolic bone diseases, including osteoporosis.

Key words : osteopetrosis, impaired bone resorption, increased bone formation, genetic disorders

* *Department of Bone and Mineral Research Osaka Medical Center & Research Institute for Maternal & Child Health*

Calcif Tissue Int (2012) 90:307–318
DOI 10.1007/s00223-011-9567-0

ORIGINAL RESEARCH

Skeletal Analysis of the Long Bone Abnormality (*lbab/lbab*) Mouse, A Novel Chondrodysplastic C-Type Natriuretic Peptide Mutant

Eri Kondo · Akihiro Yasoda · Takehito Tsuji · Toshihito Fujii · Masako Miura · Naotestu Kanamoto · Naohisa Tamura · Hiroshi Arai · Tetsuo Kunieda · Kazuwa Nakao

Received: 5 July 2011 / Accepted: 22 December 2011 / Published online: 25 January 2012

Abstract Long bone abnormality (*lbab/lbab*) is a strain of dwarf mice. Recent studies revealed that the phenotype is caused by a spontaneous mutation in the *Nppc* gene, which encodes mouse C-type natriuretic peptide (CNP). In this study, we analyzed the chondrodysplastic skeletal phenotype of *lbab/lbab* mice. At birth, *lbab/lbab* mice are only slightly shorter than their wild-type littermates. Nevertheless, *lbab/lbab* mice do not undergo a growth spurt, and their final body and bone lengths are only ~60% of those of wild-type mice. Histological analysis revealed that the growth plate in *lbab/lbab* mice, especially the hypertrophic chondrocyte layer, was significantly thinner than in wild-type mice. Overexpression of CNP in the cartilage of *lbab/lbab* mice restored their thinned growth plate, followed by the complete rescue of their impaired endochondral bone growth. Furthermore, the bone volume in *lbab/lbab* mouse was severely decreased and was recovered by CNP overexpression. On the other hand, the thickness of the growth plate of *lbab/+* mice was not different from that of wild-type mice; accordingly, impaired endochondral bone growth was not observed in *lbab/+* mice. In organ culture experiments, tibial explants from fetal *lbab/lbab* mice were significantly shorter than those from *lbab/+* mice and elongated by addition of 10^{-7} M CNP to the same extent as *lbab/+* tibiae treated with the same dose of CNP. These results demonstrate that *lbab/lbab* is a novel mouse model of chondrodysplasia caused by insufficient CNP action on endochondral ossification.

Keywords C-type natriuretic peptide · Long bone abnormality (*lbab*) · Chondrodysplasia · Endochondral bone growth · Organ culture

C-type natriuretic peptide (CNP) is a member of the natriuretic peptide family and exerts its biological actions through the accumulation of intracellular cyclic GMP via a subtype of membranous guanylyl cyclase receptor, guanylyl cyclase-B (GC-B) [1, 2]. We previously demonstrated that the CNP/GC-B system is a potent stimulator of endochondral bone growth: transgenic mice with targeted overexpression of CNP in cartilage under the control of type II collagen promoter [3] or those with elevated plasma CNP concentrations under the control of human serum amyloid P component promoter [4] exhibit a prominent skeletal overgrowth phenotype. On the other hand, the physiological importance of the CNP/GC-B system on endochondral bone growth has been revealed by the phenotypes of hypomorphs. We generated complete CNP or GC-B null mice and demonstrated that they exhibit an impaired bone growth phenotype [5, 6]. We have also reported that in two lines of spontaneous mutant mice, *cn/cn* and *slw/slw*, disproportionate dwarfism is caused by loss-of-function mutations in the murine GC-B gene [7, 8].

The authors have stated that they have no conflict of interest.

Electronic supplementary material The online version of this article (doi:10.1007/s00223-011-9567-0) contains supplementary material, which is available to authorized users.

E. Kondo · A. Yasoda (✉) · T. Fujii · M. Miura · N. Kanamoto · N. Tamura · H. Arai · K. Nakao
Department of Medicine and Clinical Science, Kyoto University Graduate School of Medicine, Kyoto 606-8507, Japan
e-mail: yasoda@kuhp.kyoto-u.ac.jp

T. Tsuji · T. Kunieda
Department of Animal Science, Okayama University Graduate School of Natural Science and Technology, Okayama 700-8530, Japan

The skeletal phenotypes of these mutant mice resemble those of GC-B knockout mice. Furthermore, recent studies have elucidated that loss-of-function mutations in the human GC-B gene are the causes of acromesomelic dysplasia type Maroteaux (AMDM), one form of skeletal dysplasia with a disproportionate short stature phenotype [9]. The impaired skeletal growth phenotype observed in patients suffering from AMDM is similar to the skeletal phenotype of *cn/cn*, *slw/slw*, and GC-B knockout mice.

The long bone abnormality (*lbab/lbab*) mouse was first identified in The Jackson Laboratory (Bar Harbor, ME) as a spontaneous autosomal recessive mutant characterized by impaired growth of the long bones [10]. Recent studies have elucidated that the impaired growth of *lbab/lbab* mice is caused by a hypomorphic mutation in the CNP gene; Jiao et al. [11] found that its impaired growth phenotype is associated with a single point mutation in the mouse CNP gene, and we showed that this phenotype is completely recovered by CNP overexpression [12]. Yoder et al. [13] characterized the mutant CNP in *lbab/lbab* mice and demonstrated that it is less biologically active than authentic CNP; in whole-cell cGMP elevation and membrane guanylyl cyclase assays, 30-fold to greater than 100-fold more mutant CNP is required to activate GC-B compared to authentic CNP. We also confirmed that the mutant CNP in *lbab/lbab* mice retains only about 10% activity to induce cyclic GMP production through GC-B compared to authentic CNP in an in vitro transfection assay using COS-7 cells [12]. Collectively, *lbab/lbab* is a novel chondrodysplastic mouse model with insufficient CNP action on endochondral bone growth. Nevertheless, the skeletal phenotypes of *lbab/lbab* mice have only been partially described in short reports, including our own brief communication [11–13], and have not yet been fully studied. In this study, we performed further analyses of the skeletal phenotypes of *lbab/lbab* mice.

Materials and Methods

Mice

Heterozygous (*lbab/+*) mice (C57BL/6 J background) were obtained from The Jackson Laboratory, and the strain was maintained by sib mating of heterozygotes. Transgenic mice with targeted overexpression of CNP in the growth plate chondrocytes under the control of the mouse pro-α_1(II) (*Col2a1*) promoter (CNP-Tg) were created as reported previously [3]. To perform genetic rescue of *lbab/lbab* mice, CNP-Tg mice were mated with *lbab/+* mice, and F_1 offspring heterozygous for the transgene and for the *lbab* allele were mated with those with only the *lbab* allele to generate *lbab/lbab* mice with the transgene expression (*lbab/lbab*·CNP-Tg/+ mice) [12]. Genotypes for the CNP transgene and the *lbab* allele were determined by PCR analysis using mouse genomic DNAs extracted from tails. Because there was no tendency of gender differences in the growth of each genotype (data not shown), we used only female mice in our experiments. Animal care and all experiments were conducted in accordance with the Guidelines for Animal Experiments of Kyoto University and were approved by the Animal Research Committee, Graduate School of Medicine, Kyoto University.

Skeletal Analysis

For 10 weeks after birth, body lengths of female mice were measured weekly. Body length was measured as the length from the nose to the anus (nasoanal length) or that from the nose to the tip of the tail (nose–tail length). Body weights were also measured weekly. Skeletal analysis was performed as previously described [14]. Briefly, mice were subjected to soft X-ray analysis (30 kVp, 5 mA for 1 min; Softron type SRO-M5; Softron, Tokyo, Japan), and lengths of the bones were measured on the X-ray films. CT scanning of the humerus was performed using a ScanXmate-L090 Scanner (Comscantechno, Yokohama, Japan). Three-dimensional microstructural image data were reconstructed and structural indices calculated using TRI/3D-BON software (RATOC System Engineering, Tokyo, Japan).

Histological Examination

Tibiae were fixed in 10% formalin neutral buffer, decalcified in 10% EDTA, and embedded in paraffin. Sections (5 μm thick) were sliced and stained with alcian blue (pH 2.5) and hematoxylin–eosin. For immunohistochemistry, sections were incubated with rabbit anti-type X collagen antibody (LSL, Tokyo, Japan), goat anti-Indian hedgehog (Ihh) antibody (Santa Cruz Biotechnology, Santa Cruz, CA), mouse anti-matrix metalloproteinase 13 (MMP-13) antibody (Thermo Fisher Scientific, Waltham, MA), and mouse anti–proliferating cell nuclear antigen (PCNA) antibody (Dako, Copenhagen, Denmark). Immunostaining was performed using the Histofine Mousestain Kit (Nichirei Biosciences, Tokyo, Japan) according to the manufacturer's instruction. Peroxidase activity was visualized using diaminobenzidine. Sections were counterstained with hematoxylin, dehydrated, and then mounted with malinol (Muto Pure Chemicals, Tokyo, Japan). To confirm antibody specificity, normal rabbit serum (Sigma-Aldrich, St. Louis, MO), normal goat IgG (Santa Cruz Biotechnology), and mouse IgG (Dako) were used as first antibodies for negative controls.

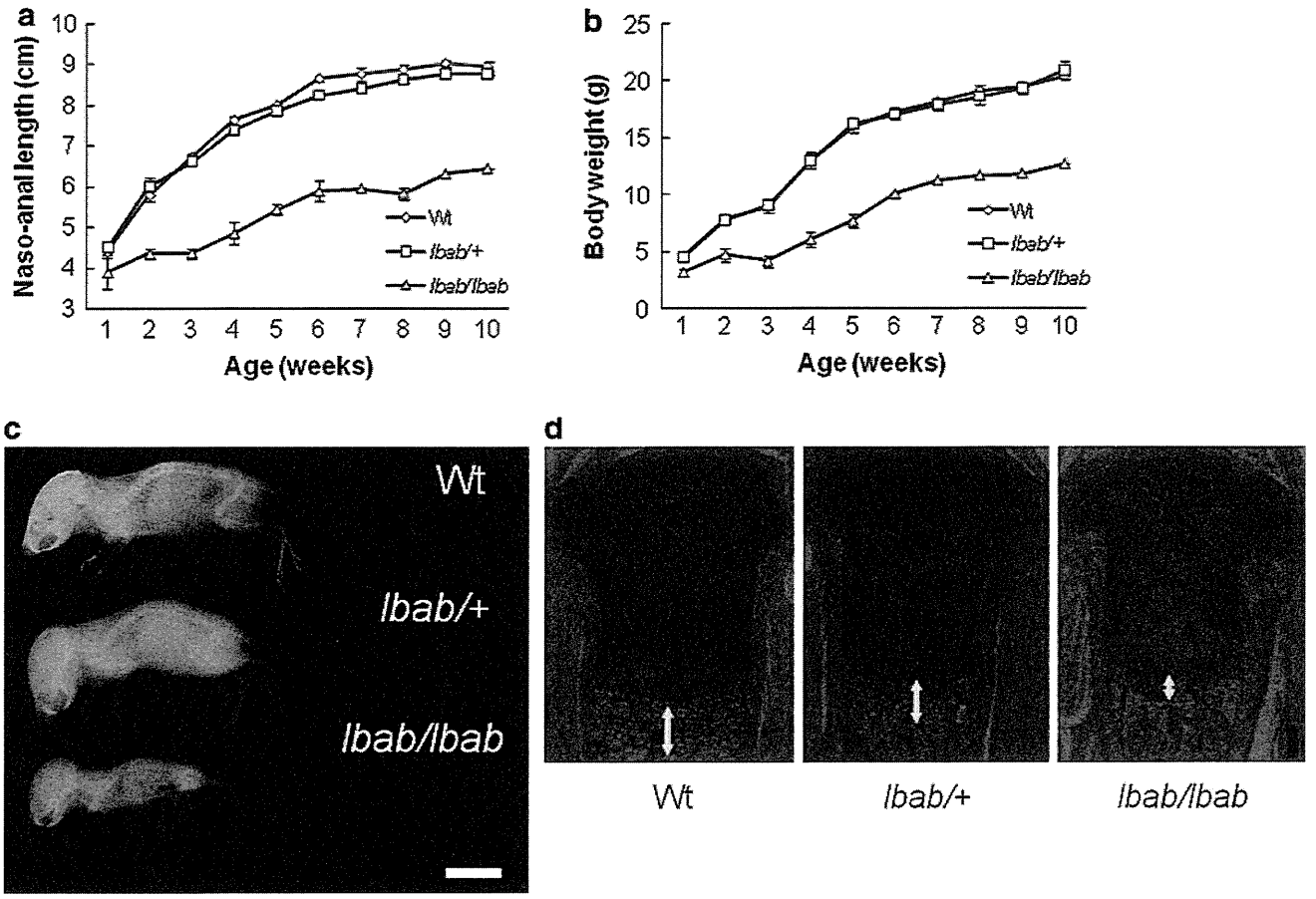

Fig. 1 Growth and skeletal phenotype of *lbab/+* and *lbab/lbab* mice. Nasoanal lengths (**a**) and body weights (**b**) of female wild-type (*Wt, open diamond*), *lbab/+* (*open square*), and *lbab/lbab* (*open triangle*) mice (n = 2–8). **c** Whole skeletons of wild-type, *lbab/+* , and *lbab/lbab* mice at 2 weeks of age. *Scale bar* 1 cm. **d** Histological analysis of the tibial growth plates of 3-day-old mice. *Arrows* indicate hypertrophic chondrocyte layers. Alcian blue and hematoxylin–eosin staining. *Scale bar* 100 μm

Organ Culture

Organ culture of fetal mouse tibiae or third metatarsi was performed as described previously [15]. Tibial or metatarsal explants from *lbab/+* mice and their *lbab/lbab* littermates at 16.5 days postcoitus were cultured for 4 days with vehicle or 10^{-7} M CNP (Peptide Institute, Minoh, Japan). Medium was changed every day. Before and after the culture, the maximal longitudinal lengths of tibiae were measured as the total tibial length, the sum of the lengths of proximal and distal cartilaginous primordia (CP), and the length of the osteogenic center (OC), using a linear ocular scale mounted on an inverted microscope. For histological analysis, explants were fixed in 10% formalin neutral buffer and embedded in paraffin. Sections (5 μm thick) were sliced and stained with alcian blue (pH 2.5) and hematoxylin–eosin. Immunohistochemical staining of incorporated bromodeoxyuridine (BrdU) was performed using 5-Bromo-2′-deoxyuridine labeling and detection kit II (Roche Applied Science, Indianapolis, IN) according to the manufacturer's protocol.

Statistical Analysis

Data were expressed as the mean ± SEM. The statistical significance of differences between mean values was assessed using Student's t-test.

Results

Analyses of Skeletal Growth of *lbab/lbab* and *lbab/+* Mice

As previously reported, *lbab/lbab* mice developed severe dwarfism characterized by short tails and extremities [11, 12]. At birth, *lbab/lbab* pups were slightly shorter than their wild-type littermates: the nasoanal and nose–tail lengths of *lbab/lbab* mice were 88 and 83% of those of

their wild-type littermates, respectively (Fig. 1a, Supplemental Fig. 1).The ratios of nasoanal and nose–tail lengths of *lbab/lbab* mice to those of wild-type mice sharply decreased to 65% and 55%, respectively, by the age of 3 weeks. After 5 weeks of age, these ratios stabilized at 66–72% and 57–62%, respectively (Fig. 1a, Supplemental Fig. 1). The body weight of *lbab/lbab* mice was 68% of that of their wild-type littermates at birth and decreased to 46% by the age of 3 weeks. The ratio did not increase until 5 weeks of age, becoming ~60% after 7 weeks (Fig. 1b). On the other hand, *lbab/+* mice were indistinguishable from their wild-type littermates at birth and grew almost similarly (Fig. 1a,b, Supplemental Fig. 1). Soft X-ray analysis revealed that longitudinal growth of the vertebrae, tail, and extremities was affected in *lbab/lbab* mice at the age of 2 weeks but was not affected in *lbab/+* mice (Fig. 1c). Histological analysis revealed that at the age of 3 days the tibial growth plate, especially the hypertrophic chondrocyte layer, of *lbab/lbab* mice was apparently thinner than that of wild-type mice (Fig. 1d). On the other hand, the thickness of the tibial growth plate of *lbab/+* mice was not different from that of wild-type mice (Fig. 1d).

Effect of CNP Overexpression on Impaired Endochondral Bone Growth of *lbab/lbab* Mice

In order to further characterize the impaired skeletal growth of *lbab/lbab* mice, we analyzed how their impaired endochondral bone growth recovered in response to targeted overexpression of CNP in the cartilage in vivo [12]. We crossed *lbab/lbab* mice with cartilage-specific CNP transgenic mice under the control of type II collagen promoter (CNP-Tg mice) and obtained *lbab/lbab* mice with transgenic expression of CNP in cartilage (*lbab/lbab*·CNP-Tg mice) [12]. At the first week after birth, the nasoanal length of *lbab/lbab*·CNP-Tg mice was almost the same as that of *lbab/lbab* mice and considerably smaller than that of wild-type mice: nasoanal lengths of wild-type, *lbab/lbab*, and *lbab/lbab*·CNP-Tg mice were 4.38 ± 0.06, 3.87 ± 0.37, and 4.00 ± 0.12 cm, respectively. Subsequently, *lbab/lbab*·CNP-Tg mice began to grow larger than *lbab/lbab* mice and promptly caught up with wild-type mice; although the nasoanal length of *lbab/lbab*·CNP-Tg mice was still considerably smaller than that of wild-type mice until 3 weeks of age (5.70 ± 0.57 and 6.71 ± 0.10 cm, respectively, at age 3 weeks), it became almost comparable to that of wild-type mice after 4 weeks (7.38 ± 0.48 and 7.61 ± 0.10 cm, respectively, at age 4 weeks). Further, the body weight of *lbab/lbab*·CNP-Tg mice was almost the same as that of *lbab/lbab* mice and smaller than that of wild-type mice until the age of 3 weeks but then promptly increased to a level comparable to that of wild-type mice (Supplemental Fig. 2).

Soft X-ray analyses revealed that at the age of 2 weeks the impaired growth of bones formed through endochondral ossification in *lbab/lbab* mice was partially recovered by targeted overexpression of CNP in cartilage in *lbab/lbab*·CNP-Tg mice (Fig. 2a): the recoveries in the longitudinal length of cranium and the lengths of the humerus, radius, ulna, femur, tibia, and vertebrae were 35, 73, 68, 37, 51, 63, and 27%, respectively (Fig. 2b). Furthermore, at the age of 10 weeks, the impaired endochondral bone growth in *lbab/lbab* mice was almost completely recovered by targeted overexpression of CNP in cartilage, as observed in *lbab/lbab*·CNP-Tg mice (Fig. 2c, d). On the other hand, there were no significant differences in the width of the cranium, which is formed via intramembranous ossification, among the three genotypes at either 2 or 10 weeks (Fig. 2b, d).

Histological analysis showed that the thickness of both the proliferative chondrocyte layer and the hypertrophic chondrocyte layer, positive for immunohistochemical staining for type X collagen, was significantly decreased in *lbab/lbab* mice compared to wild-type mice at the age of 2 weeks, as previously reported [12] (Fig. 3a, b).The thinner proliferative chondrocyte layer in the *lbab/lbab* growth plate was completely recovered by targeted overexpression of CNP as observed in the *lbab/lbab*·CNP-Tg growth plate (Fig. 3c). The thinner hypertrophic chondrocyte layer in the *lbab/lbab* growth plate was also considerably recovered in the *lbab/lbab*·CNP-Tg growth plate, although the extent of the recovery was less than in the proliferative chondrocyte layer (Fig. 3d). Immunohistochemical staining for PCNA revealed that the number of PCNA-positive cells was severely decreased in the proliferative chondrocyte layer of the *lbab/lbab* growth plate (Fig. 3e). The number of PCNA-positive cells did not recover in the proliferative chondrocyte layer of the *lbab/lbab*·CNP-Tg growth plate, whereas the thinner proliferative chondrocyte layer in the *lbab/lbab* growth plate was almost completely recovered in the *lbab/lbab*·CNP-Tg growth plate (Fig. 3c). The area positive for immunostaining of Ihh, one of the markers of hypertrophic differentiation, was decreased in the *lbab/lbab* growth plate compared to the wild-type growth plate (Fig. 3f). The smaller size of the area positive for Ihh in the *lbab/lbab* growth plate was almost completely recovered in the *lbab/lbab*·CNP-Tg growth plate (Fig. 3f). Immunohistochemical staining of MMP-13, a useful marker for terminal hypertrophic chondrocytes, was not changed between the three genotypes, indicating that the progression through the hypertrophy program was not accelerated in the *lbab/lbab* growth plate (Fig. 3g).

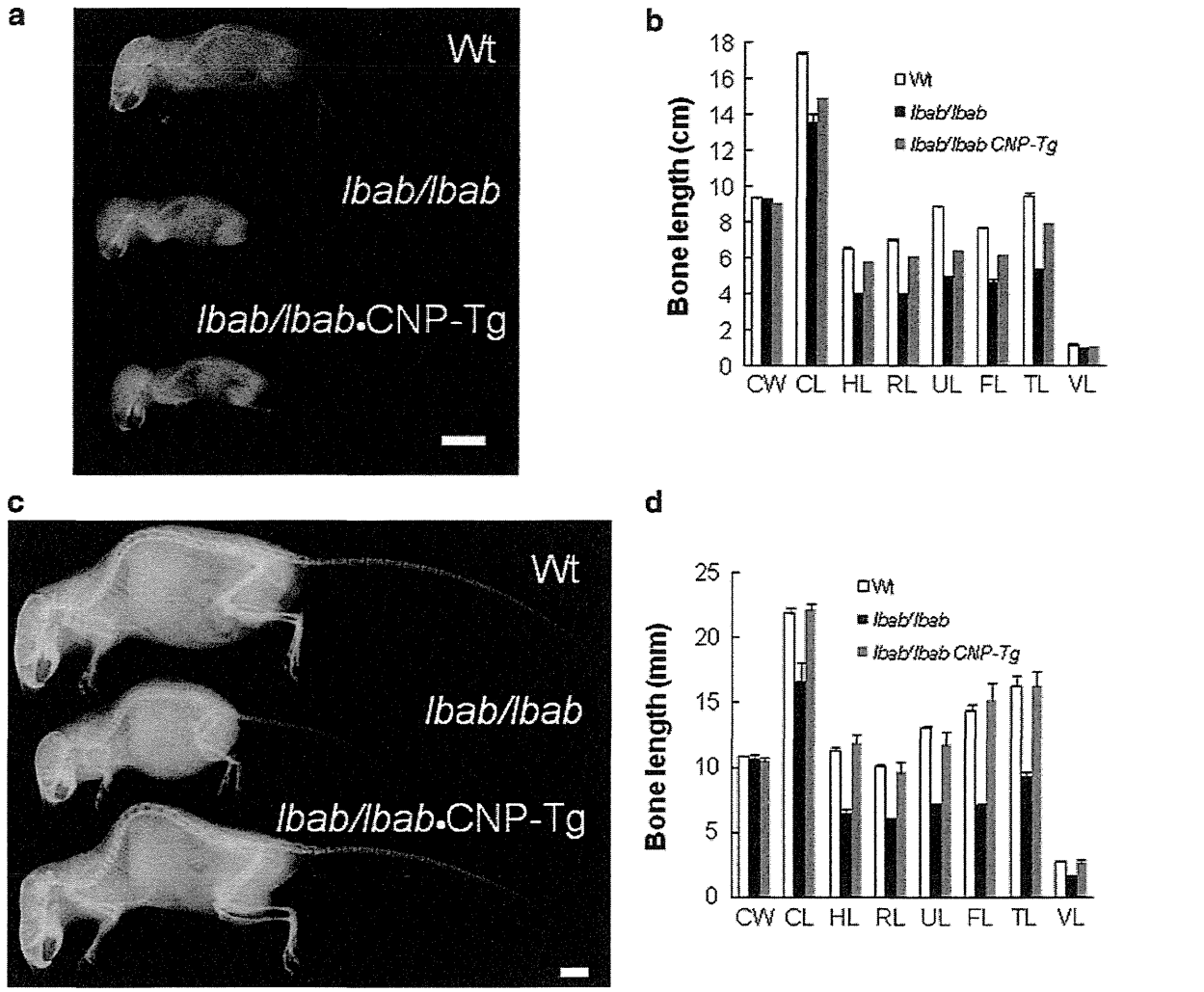

Fig. 2 Effect of CNP overexpression on impaired endochondral bone growth of *lbab/lbab* mice. Whole skeletons (**a**, **c**) and bone lengths measured on soft X-ray films (**b**, **d**) of female wild-type (*Wt*), *lbab/lbab*, and *lbab/lbab*·CNP-Tg mice at the age of 2 weeks (**a**, **b**) and 10 weeks (**c**, **d**). **a**, **c** *Scale bar* 1 cm. **b**, **d** *White bars*, wild-type mice; *black bars*, *lbab/lbab* mice; *gray bars*, *lbab/lbab*·CNP-Tg mice. *CW*, width of cranium; *CL*, longitudinal length of cranium; *HL*, humeral length; *RL*, radial length; *UL*, ulnar length; *FL*, femoral length; *TL*, tibial length; *VL*, vertebral length. $n = 2$–7 (**b**) and 3–5 (**d**) (Color figure online)

At the age of 10 weeks, the tibial growth plate of *lbab/lbab* mice continued to be thinner than that of wild-type mice and was completely recovered by overexpression of CNP in cartilage (Fig. 4).

Recovery of Decreased Bone Volume in *lbab/lbab* Mouse by CNP Overexpression

Three-dimensional CT analysis manifested a marked reduction in bone volume of the humerus in *lbab/lbab* mice and considerable recovery in *lbab/lbab*·CNP-Tg mice (Fig. 5). At the age of 10 weeks, the quantified bone volume (BV/TV) and trabecular thickness (Tb.Th) of the humerus in *lbab/lbab* mice were 2.4% and 34.5 μm, whereas those in wild-type mice were 4.1% and 40.3 μm, respectively. The decreased BV/TV and Tb.Th in *lbab/lbab* mice were increased to 5.4% and 37.0 μm, respectively, in *lbab/lbab*·CNP-Tg mice.

Organ Culture Experiments of Tibiae from *lbab/lbab* Mice

In order to further analyze the impaired endochondral ossification of *lbab/lbab* mice, we preformed organ culture experiments using tibial explants from fetal mice (Fig. 6a) [15]. Because skeletal phenotypes of mice heterozygous for the *lbab* allele were not different from those of wild-type mice, we compared the growth of tibial explants from *lbab/lbab* mice with that from *lbab/+* mice. At the beginning of culture, both the total length and the sum length of the CP of *lbab/lbab* tibiae were significantly smaller than those of *lbab/+* tibiae (3.80 ± 0.04

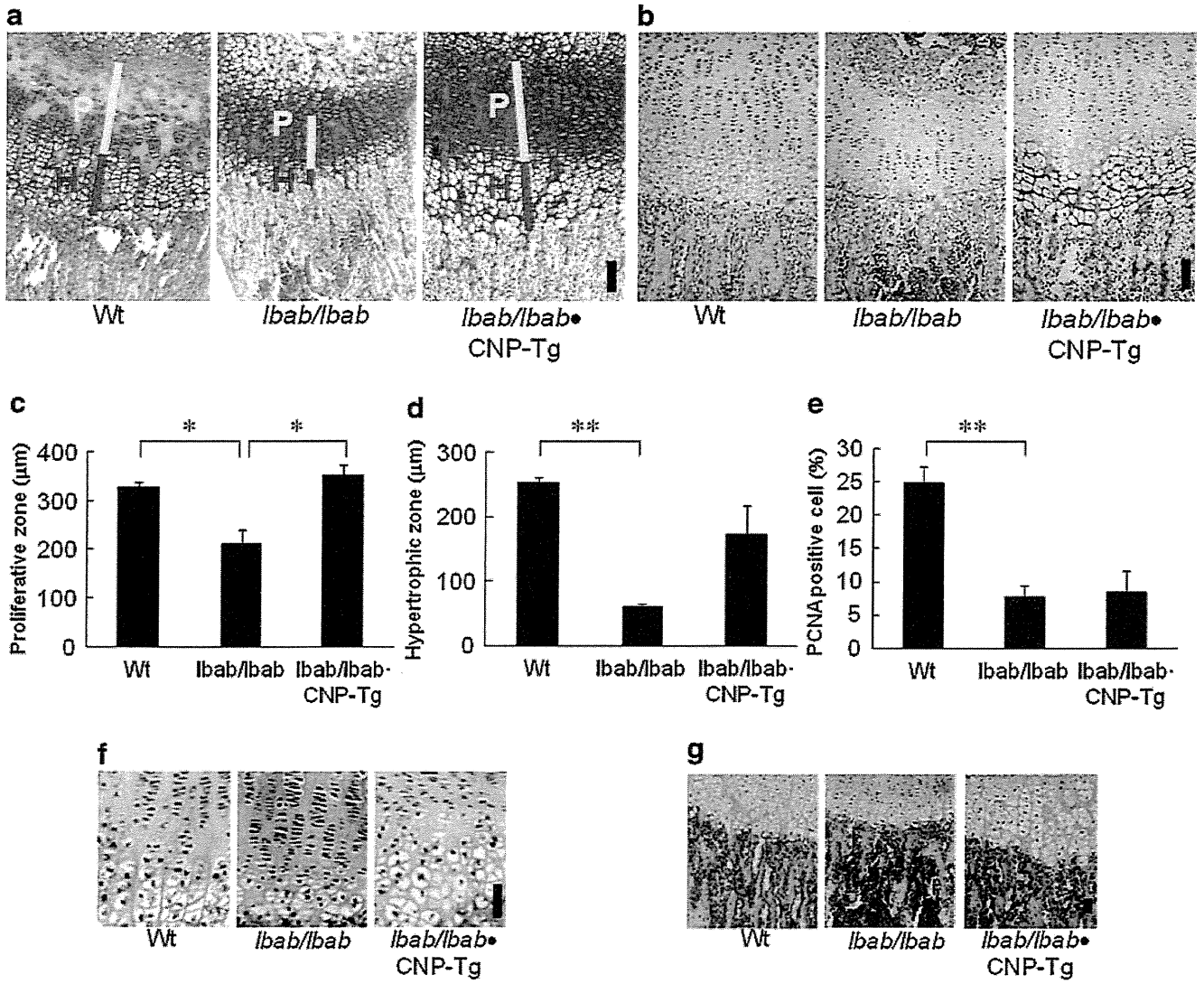

Fig. 3 Histological analysis of tibial growth plates from 2-week-old wild-type (*Wt*), *lbab/lbab*, and *lbab/lbab*·CNP-Tg mice. **a** Alcian blue and hematoxylin–eosin staining. *Yellow bars* (depicted as *P*) indicate proliferative chondrocyte layers, and *red bars* (depicted as *H*) indicate hypertrophic chondrocyte layers. **b** Immunohistochemical staining for type X collagen. Scale bar in **a** and **b** = 100 μm. Heights of the proliferative (**c**) and hypertrophic (**d**) chondrocyte layers. $n = 3$ each. $^{*}P < 0.05$, $^{**}P < 0.01$. **e** The proportion of PCNA-positive chondrocytes in proliferative chondrocyte layers. $n = 3$–4. $^{**}P < 0.01$. Immunohistochemical staining of Ihh (**f**) and MMP-13 (**g**). Scale bar in **f** and **g** = 50 μm

vs. 4.25 ± 0.03 and 2.19 ± 0.02 vs. 2.43 ± 0.01 mm, respectively, $n = 8$–12 each) (Fig. 6b, c). Tibial explants from *lbab/lbab* mice grew to the same extent as those from *lbab/+* mice during a 4-day culture period; the difference in the total length or in the length of the CP between *lbab/lbab* and *lbab/+* explants at the end of culture was comparable to that at the beginning of culture (Fig. 6b, c). There was no significant difference in the length of the OC between the two genotypes before and after the culture period (data not shown).

The treatment of CNP at the dose of 10^{-7} M stimulated the growth of both *lbab/lbab* and *lbab/+* tibiae (Fig. 6b, c). CNP stimulated the growth of *lbab/lbab* tibiae more potently than that of *lbab/+* tibiae; in the presence of 10^{-7} M CNP, the difference between the total length of *lbab/+* tibiae and that of *lbab/lbab* tibiae was decreased (Fig. 6b), and furthermore, the CP length of *lbab/lbab* tibiae became almost the same as that of *lbab/+* tibiae (Fig. 6c). The growth of the OC was not stimulated by CNP in either *lbab/lbab* or *lbab/+* explants (data not shown).

Histological examination at the end of the culture period revealed that the length of the primordial growth plate (Fig. 7a), especially that of the hypertrophic chondrocyte layer positive for type X collagen immunostaining (Fig. 7b,c), was smaller in *lbab/lbab* explants than in

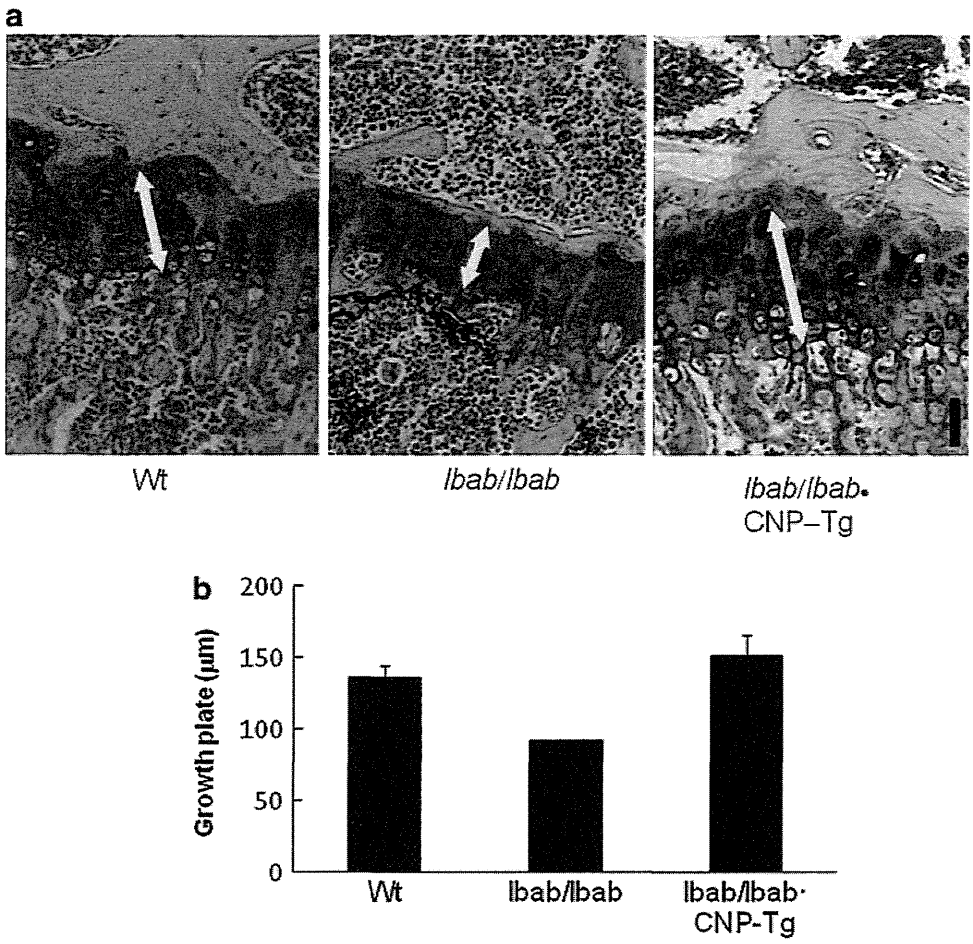

Fig. 4 Histological analysis of tibial growth plate from female 10-week-old wild-type (*Wt*), *lbab/lbab*, and *lbab/lbab*-CNP-Tg mice. **a** Alcian blue and hematoxylin–eosin staining. *Arrows* indicate the width of growth plates. *Scale bar* 50 μm. **b** Total heights of the growth plates. $n = 2$–5 each

lbab/+ explants. The area positive for immunostaining for Ihh, one of the markers for chondrogenic differentiation [16], tended to be a little decreased in *lbab/lbab* explants compared to that in *lbab*/+ explants, although the intensity of the immunostaining was not different between the two genotypes (Supplemental Fig. 3). Immunohistochemical detection of BrdU-incorporated chondrocytes revealed that BrdU-positive chondrocytes tended to be decreased in *lbab/lbab* explants compared to those in *lbab*/+ explants (Fig. 7d). Addition of CNP prominently increased the lengths of primordial growth plates (Fig. 7a) and their hypertrophic chondrocyte layers (Fig. 7b, c) of both *lbab*/+ and *lbab/lbab* explants. The lengths of the primordial growth plate and its hypertrophic chondrocyte layer of *lbab/lbab* explants treated with 10^{-7} M CNP became comparable to those of *lbab*/+ explants treated with the same dose of CNP (Fig. 7a–c). CNP increased the areas positive for Ihh immunostaining in both *lbab*/+ and *lbab/lbab* explants. By addition of CNP, the sizes of the areas positive for, and the intensities of, Ihh immunostaining were not different between *lbab*/+ and *lbab/lbab* explants (Supplemental Fig. 3). CNP did not increase BrdU-positive chondrocytes in *lbab/lbab* explants (Fig. 7d).

Further, we explored whether CNP controls the progression of growth plate chondrocytes through the different stages of maturation or not. Because the process of endochondral ossification is delayed in the metatarsus compared to that in the tibia in an individual, we performed organ culture of metatarsi as well as tibiae from fetal mice at 16.5-days postcoitus and examined the expression of type X collagen and Ihh. In the case of *lbab*/+ organ culture, the area positive for immunostaining of type X collagen was reduced and that of Ihh was localized near the ossification center in metatarsal explants compared with those in tibial explants, indicating that the metatarsal growth plate represents an earlier stage of endochondral ossification than the tibial growth plate (Fig. 8). The area positive for immunostaining of type X collagen was greatly reduced in *lbab/lbab* metatarsal explants compared with that in *lbab*/+ metatarsal explants and recovered by addition of 10^{-7} M CNP to the same extent to that in *lbab*/+ metatarsal explants treated with vehicle. The area positive for immunostaining of Ihh became closer to ossification center

Fig. 5 Micro-CT analysis of humeri from wild-type (*Wt*), *lbab/lbab*, and *lbab/lbab*·CNP-Tg mice at the age of 10 weeks. *Scale bar* 1 mm

in *lbab/lbab* metatarsal explants than in *lbab/+* metatarsal explants and was returned to the same position as *lbab/+* metatarsal explants by addition of CNP (Fig. 8).

Discussion

Previously, we and other groups had reported in brief communications that the short stature phenotype of *lbab/lbab* mice is caused by a mutation in the CNP gene [11–13]. Here, we further analyzed the skeletal phenotypes of *lbab/lbab* mice and report the results in this full-length article.

Analysis of the growth curves of nasoanal and nose–tail lengths revealed that the shortness of *lbab/lbab* mice is mild at birth but rapidly progresses by the age of 3 weeks, and then, after 4 weeks, the ratio of the length of *lbab/lbab* mice compared to that of wild-type mice becomes almost constant. This suggests that CNP is especially crucial for the skeletal growth spurt that occurs in early life. Since CNP is expressed in the growth plate cartilage and works as an autocrine/paracrine regulator [5], CNP might affect the endochondral bone growth potently when the volume of growth plate cartilage is relatively abundant.

We confirmed the thinness of the growth plate of *lbab/lbab* mice, especially in its hypertrophic chondrocyte layer, followed by the impaired growth of long bones. The thinness of the growth plate of *lbab/lbab* mice was almost completely recovered by targeted overexpression of CNP in the growth plate by the age of 2 weeks. On the other hand, the recovery of the shortness of the total length of *lbab/lbab* bones by CNP was only partial at 2 weeks, becoming complete at the age of 10 weeks. This finding suggests that the recovery is evident earlier in the thickness of the growth plate than in the total bone length. In addition, immunohistochemistry for PCNA revealed that at the age of 2 weeks the proliferation of growth plate chondrocytes is decreased in *lbab/lbab* mice and that the decreased proliferation is not rescued by CNP overexpression, even though the thickness of the growth plate does fully recover.